Bleaching and Degradation of Textile Dyes by Nonthermal Plasma Process at Atmospheric Pressure

5 AUTHORS, INCLUDING:

Fatiha Abdelmalek
Université Abdelhamid Ibn Badis Mostaganem
34 PUBLICATIONS   **572** CITATIONS

SEE PROFILE

Ghezzar Mouffok Redouane
Université Abdelhamid Ibn Badis Mostaganem
14 PUBLICATIONS   **150** CITATIONS

SEE PROFILE

Ahmed Addou
Université Abdelhamid Ibn Badis Mostaganem
80 PUBLICATIONS   **961** CITATIONS

SEE PROFILE

Ind. Eng. Chem. Res. **2006,** *45,* 23−29

23

Bleaching and Degradation of Textile Dyes by Nonthermal Plasma Process at Atmospheric Pressure

Fatiha Abdelmalek,[†,‡] **Mouffok R. Ghezzar,**[†] **Mohamed Belhadj,**[†] **Ahmed Addou,**[†] **and Jean-Louis Brisset*,**[‡]

Laboratoire des Sciences et Techniques de l'Environnement et de la Valorisation. Faculté des Sciences de l'Ingénieur, Université de Mostaganem, Mostaganem, Algérie, and Laboratoire d'Electrochimie Interfaciale et de Chimie Analytique. Faculté des Sciences, Université de Rouen. 76821 Mont Saint-Aignan Cedex; France

The degradation of aqueous solutions of various dyes (e.g., Orange I, Crystal Violet, and Eriochrome Black T) used for the textile industry was performed by means of a special nonthermal quenched plasma technique (i.e., the gliding arc technique, which results from an electric discharge at atmospheric pressure and ambient temperature). The gaseous species formed in the discharge, and especially the OH radicals, induce strong oxidizing effects in the target solution, so that bleaching of the solution and degradation of the solute result, as evidenced by absorbance and chemical oxygen demand (COD) measurements. The two processes were considered as matching reactions, and overall kinetic data were derived when possible. A tentative mechanism based on literature data is also presented.

1. Introduction

Dyes make our world beautiful, but they bring us pollution: the colored waters of industrial effluents are unattractive because they account for significant concentrations of pollutants so that they become the sources of increasingly acute complaints. In particular, the wastewaters generated by the textile industry are characterized by strong color, highly fluctuating pH, high chemical oxygen demand (COD), and biotoxicity.[1] Most of the synthetic dyes are azo dyes, and a number of them are suspected to be carcinogenic.[2,3]

The presence of dyes in water, even at very low concentrations, is easy to detect and makes the occurrence of the relevant solutes undesirable.[4,5] Color is thus among the first contaminants to be identified, so that environmental regulations in most countries have made the bleaching of textile wastewaters mandatory prior to discharge.[6]

Environmental pollution by organic dyes presents a severe ecological problem that is increased by the fact that most of these dyes are difficult to degrade by traditional techniques. Effective degradation of dye solutions has been achieved by means of advanced oxidation processes (AOPs),[7−12] which generate powerful oxidizing agents, such as hydroxyl radicals HO$^{\bullet}$ ($E^{\circ}_{OH^{\circ}/H_2O}$ = 2.8 V vs normal hydrogen electrode). These techniques have been found especially suitable for degrading azo-type dyes, which are the most-used textile colorants[13−16]

In this study, we propose an electric process that is based on using a nonthermal plasma generated by electric discharges in humid air. Hydroxyl radicals (HO$^{\bullet}$) form when the discharge burns in humid air.[17] The reactive species generated are able to degrade organic pollutants such as dyes, because the treatment consists of oxidizing destruction.[18−20] Azo dyes constitute the largest group of industrial dyes.

In the present work, we examine the degradation of two representative compounds, i.e., Orange I and Eriochrome Black

Table 1. Characteristics of the Three Dyes Used for the Experiment

dye	chemical structure	λ_{max} (nm)	M_w (g/mol)
Orange I		475	350.33
Eriochrome Black		525	462.39
Crystal Violet		588	407.99

T. For these dyes, the destruction of the azo bond (−N=N−), i.e., the chromophoric group, induces the bleaching of the solutions.

A third dye (i.e., Crystal Violet, also known as Gentian violet or hexamethylpararosaniline chloride) is also considered in this study. This cationic dye presents a different chemical structure (Table 1) and is commonly used to control fungi and intestinal parasites in humans. It is additionally employed as a germ killer for burns or for various purposes in veterinary medicine.[21] Crystal Violet is also extensively used in textile dying and paper coloration.[22]

2. Experimental Section

2.1. Materials and Methods. The tested dyes (Table 1), i.e., Orange I, Crystal Violet, and Eriochrome Black T (EBT), were

---

* To whom correspondence should be addressed. E-mail: brissjl@club-internet.fr.

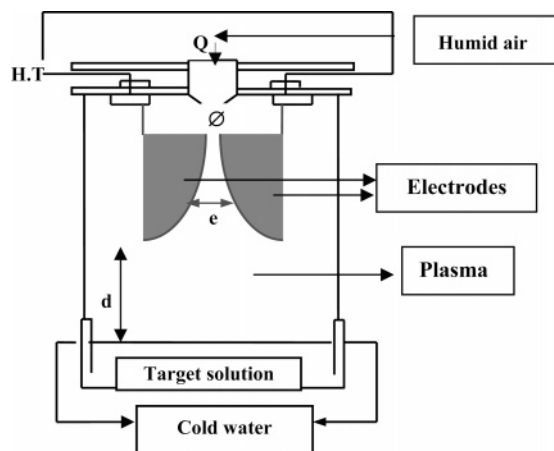† Université de Mostaganem.

‡ Université de Rouen.

Figure 1. Experimental setup.

Table 2. Properties of Dyes and Kinetics Constant of DeColorIzation and Degradation

	Orange I	Crystal Violet	Eriochrome Black T
class	acid, anionic	cationic	acid, anionic
type	azo	triphenyl	azo
C_i (mol L^{-1})	1.5×10^{-4}	1.3×10^{-4}	1.8×10^{-4}
$pH_{initial} - pH_{final}$	8.65^{-3}	$3.1^{-2.2}$	$5.1^{-2.3}$
COD (mg L^{-1})	96	153.6	144
$k_{bleaching}$ (min^{-1})	0.886	0.042	0.083
R^2	0.984	0.9947	0.9949
$k_{degradation}$ (min^{-1})	0.0173	0.024	0.0296
R^2	0.9806	0.9814	0.9995

purchased from Aldrich. They were dissolved in purified water provided by Millipore equipment. The initial concentrations of the dye solutions are reported in Table 2. All solutions were made from analytical-grade chemicals.
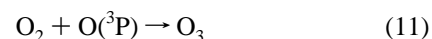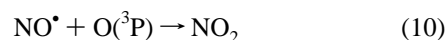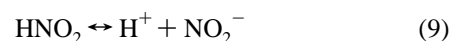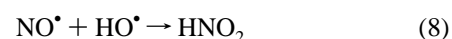
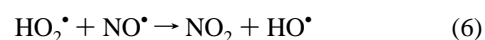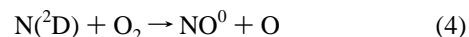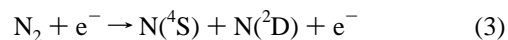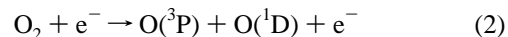The gliding arc system was described previously,[23−26] and various devices were tested for dye degradation[27] (Figure 1). Its specific use for the treatment of liquids (i.e., spent organic solvents or aqueous solutions of organic pollutants) and pollution abatement was mainly developed in our laboratory.[24,25]

An electric arc forms between two diverging electrodes raised to a convenient voltage difference (around 10 kV) at the minimum gap (i.e., few millimeters). The arc is blown by an air flow (900 L h^{-1}; nozzle diameter = 1 mm) along the axis of the system so that its feet glide along the electrodes to their tips. The arc breaks into a plume when it is short-circuited by a new arc. The resulting plasma is actually quenched plasma at atmospheric pressure and quasi-ambient temperature.

Magnetically stirred aqueous target solutions of given initial concentration (Table 2) are arrayed in front of the reactor (Figure 1), so that they can be exposed to the plasma flux for different treatment times.

Emission spectroscopy measurements on a gliding arc plasma in humid air revealed that OH• and NO• radicals are simultaneously present in the discharge with a much higher density for OH• than for NO•. The OH• radicals are responsible for the strong oxidizing properties, whereas the NO• radicals are known as parent molecules for acid derivatives HNO_2 and HNO_3, which induce acid effect.[17] The plasma plume carries away reactive species and licks the liquid surface, so that reactions can take place at the plasma−solution interface (reactions 1−11). The diffusion process in the liquid is improved by convection

in the liquid phase because of the air flow and by magnetic stirring.

$$H_2O + e^- \rightarrow H^0 + OH^0 + e^- \tag{1}$$

$$O_2 + e^- \rightarrow O(^3P) + O(^1D) + e^- \tag{2}$$

$$N_2 + e^- \rightarrow N(^4S) + N(^2D) + e^- \tag{3}$$

$$N(^2D) + O_2 \rightarrow NO^0 + O \tag{4}$$

$$H^0 + O_2 \rightarrow HO_2^{\bullet} \tag{5}$$

$$HO_2^{\bullet} + NO^{\bullet} \rightarrow NO_2 + HO^{\bullet} \tag{6}$$

$$NO_2 + HO^{\bullet} \rightarrow H^+ + NO_3^- \tag{7}$$

$$NO^{\bullet} + HO^{\bullet} \rightarrow HNO_2 \tag{8}$$

$$HNO_2 \leftrightarrow H^+ + NO_2^- \tag{9}$$

$$NO^{\bullet} + O(^3P) \rightarrow NO_2 \tag{10}$$

$$O_2 + O(^3P) \rightarrow O_3 \tag{11}$$
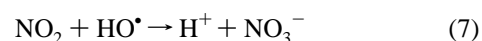
2.2. Analytical Methods. The UV−vis spectrophotometer used for the determination of dye disappearance kinetics was a Techcom 8500 spectrometer. Each plot was determined at the absorbance peak of each dye (Table 1).

The degradation kinetics was determined from the chemical oxygen demand (COD). The COD relevant to various samples and various treatment times were measured by the potassium dichromate standard method.

COD and color removal ratios (R, %) were calculated as follows

$$R_{COD} (\%) = \frac{(COD_0 - COD_i)}{COD_0} \times 100$$

where COD_0 and COD_i refer to the COD values before and after treatment, respectively, and

$$R_{color} (\%) = \frac{(ABS_0 - ABS_i)}{ABS_0} \times 100$$

where ABS is the absorbance value at the absorbance peak in the visible wavelength range; ABS_0 and ABS_i are the ABS values before and after treatment, respectively.

3. Results and Discussion

3.1. Bleaching. The colored solutions were studied by spectrophotometry measurements. The UV−vis spectrum of each dye solution was scanned, and the wavelength of the absorbance peak determined in the visible range.

When the cleavage of the −C=C− and −N=N− bonds and the aromatic rings occurs, the intensity of the absorbance peak of the polluted solution decreases. Also, the absorption band shifts from the visible to the UV or IR region of the electromagnetic spectrum, which means that the dye is degraded into lighter compounds.[28]

The UV−vis spectra obtained for all the plasma-treated dye solutions show a decrease in the intensity of the absorbance
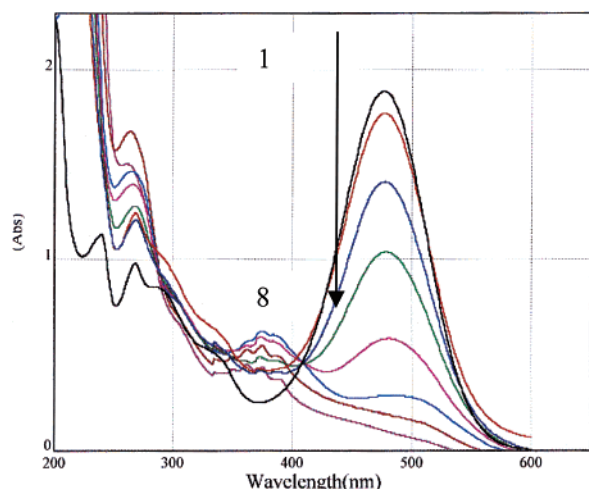
Figure 2. Spectral evolution of a plasma-treated Orange I aqueous solution (1, 0 min; 2, 1.5 min; 3, 2 min; 4, 2.5 min; 5, 3 min; 6, 3.5 min; 7, 8 min; 8, 13 min).
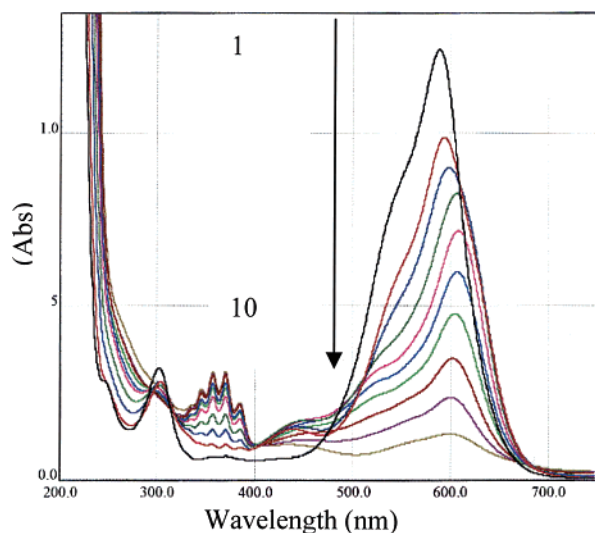

Figure 3. Spectral evolution of a plasma-treated Crystal Violet solution (1, 0 min; 2, 1 min; 3, 4 min; 4, 10 min; 5, 18 min; 6, 23 min; 7, 28 min; 8, 38 min; 9, 48 min; 10, 78 min). The particular shape of the spectra around 360 nm clearly illustrates the formation of nitrite ions.
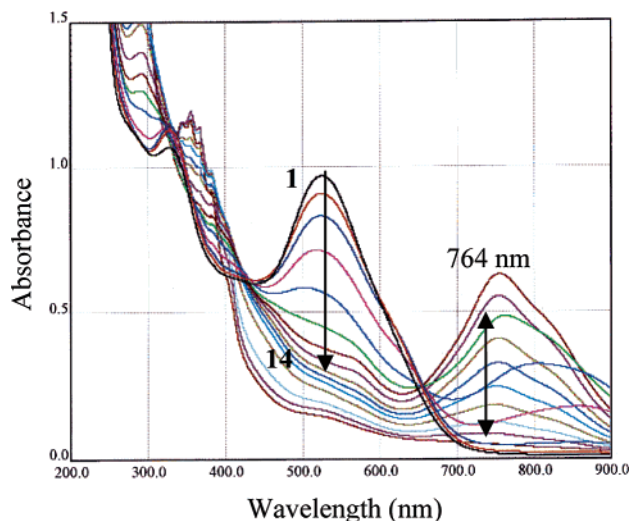

Figure 4. Spectral evolution of a plasma-treated Eriochrome Black T aqueous solution (1, 0 min; 2, 1.5 min; 3, 1.75 min; 4, 2 min; 5, 42.5 min; 6, 3.25 min; 7, 4 min; 8, 5.5 min; 9, 9 min; 10, 15 min; 11, 20 min; 12, 30 min; 13, 40 min; 14, 50 min; 15, 60 min).
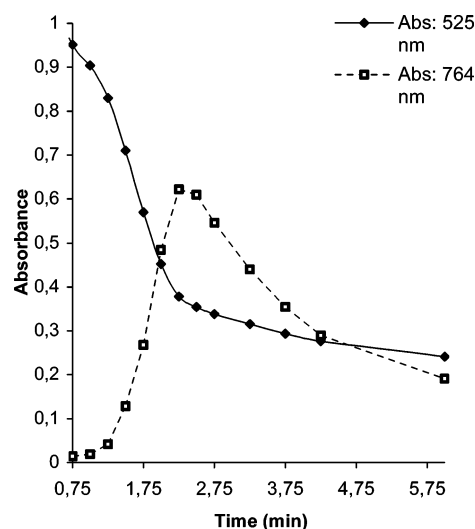

Figure 5. Formation and disappearance of Eriochrome Black T intermediate at 764 nm.

peaks at 475, 588, and 525 nm, respectively, for Orange I (Figure 2), Crystal Violet (Figure 3), and Eriochrome Black T (Figure 4). The evolution of the spectra with the treatment time of the dye solutions is more complicated in the case of EBT, because an absorption peak forms at 764 nm and later disappears. This suggests the occurrence of an intermediate compound in the general degradation scheme (Figure 5).

Exposing the azo dye solutions to the discharge first causes their fading. This is related to the breaking of the azo groups (−N=N−), which are responsible for the visible color of Orange I and EBT dyes, and to the formation of light species. The observed matching gas emission can be attributed to N_2 and related to the breaking of the nitrogen−carbon bonds close to the azo group,[29,30] although no special analysis was performed and the identification remains conjectural.

Although the absorbance peaks in the visible region of the three selected dyes disappear during the plasma treatment, new absorbance peaks around 240 nm appear in the meantime, suggesting that new species with simplified structures form.[31] For Orange I and EBT, an extra peak at 260 nm appears: it can be attributed to multisubstituted benzene rings (e.g., benzenedicarboxylic acids[32,33]) coming from the degradation of

the naphthalene ring. However, this assumption remains equivocal, because the absorption band of nitrites at $\lambda < 250$ nm might interfere with the spectra of the organic moieties.

3.1.1. Model for the Plasma−Liquid Interaction. Exposure to the plasma of the dye solutions induces a noticeable acid effect (Table 2) and the degradation of the solutes, as discussed below. The pH decrease is related to the formation in the target solution of nitrous and nitric acids, as already observed.[17,18,26] It can obviously induce color changes in the case of acid−base indicator solutions, which readily occurs at the beginning of the plasma treatment. The overall degradation process of the dye solutions involves two main parallel steps: (a) the bleaching of the treated solution with the formation of light intermediates and (b) the oxidation of the organic light solutes to carbon dioxide and water.

The second step (step b) is assumed to be less rapid than step a, and it was studied by COD measurements.

The kinetics of the bleaching step results from absorbance measurements at the main absorption peak for each dye and concerns short plasma treatment. It concerns the dye molecules, i.e., the chromophoric groups, and we can assume that the dye concentration corresponds to that of the chromophoric group.
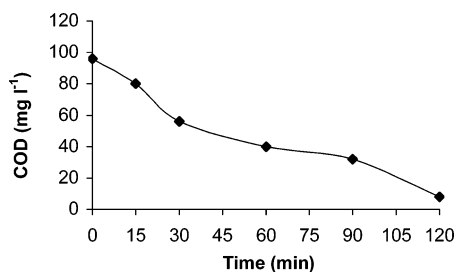
Figure 6. COD abatement of Orange I solution during the gliding arc treatment.

Hence, the overall bleaching reaction kinetic law can be written as

$$-\frac{dC_{dye}}{dt} = k_1 C_{dye}{}^{\alpha}$$

At the beginning of the treatment, all of the impinging species of the plasma attack the dye molecules present at the liquid surface, and the rate is limited by the surface concentration of the dye, which can be considered as roughly constant ($\alpha = 0$). In this case, the concentration of the solute is rather high, and the process obeys an overall zeroth-order kinetic law, as it does for the plasma treatment of pure organic spent solvents. Such situations have already been studied.[24,25]

For *dilute* organic targets or when a significant portion of the target molecules is already degraded, all of the impinging species no longer react at the target molecules, and only part of the species is efficient. The rate is then limited by the concentration of the target molecules at the surface ($\alpha = 1$) and hence by the diffusion process of the solute to the surface. The relevant kinetics then obeys a first-order law.

In the present study, the starting concentrations are rather low (Table 2), and despite the large size of the target molecules, it is reasonable to consider a first-order kinetic law as a first approximation. The relevant integrated $\ln(C_{dye}/(C_{dye}{}^0) = -k_1 t$ form accounts for a line for the matching plot $\ln C = f(t)$.

3.1.2. Bleaching Kinetics. For Orange I, the bleaching rate actually obeys a first-order reaction for $t > 1.5$ min, with a kinetic constant 0.886 min^{-1} (14.8×10^{-3} s^{-1}). However, the reaction does not start when the discharge is switched on, but requires a 1.5-min lag. Such a feature is not unique and has been observed for the plasma degradation of spent solvents. It can be tentatively related to the idea of dose (or energy threshold): a certain amount of impinging species (or the corresponding energy) is necessary to initiate the reaction.

The behaviors of the other dyes, EBT and Crystal Violet, are similar to that of Orange I. The kinetics of the bleaching reaction are first observed and obey a first-order law with the constants $k = 0.083$ min^{-1} for EBT and $k = 0.042$ min^{-1} for Crystal Violet (Table 2).

3.2. Degradation. The degradation of the dyes can be followed by measurements of the chemical oxygen demand, which is an index for the pollutant concentration in the considered solution.[34] COD indicates the degree to which degradation or mineralization of organic species has occurred.[35−38] The plasma treatment of dye solutions leads to a gradual decrease in the chemical oxygen demand (COD) as the exposure time to the discharge increases (Figures 6−8). This accounts for a degradation process of the solutes and consequently for the detoxication level of water.[34,39] The COD removals of Orange I, Crystal Violet, and Eriochrome Black T are 92%, 75%, and 83%, respectively, after a 120-min treatment.
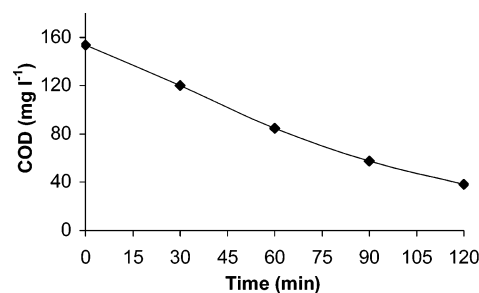

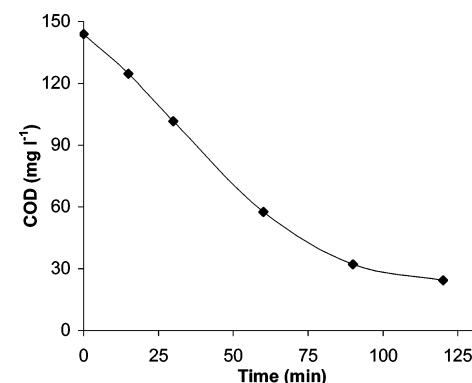**Figure 7.** COD abatement of Crystal Violet solution during the gliding arc treatment.

Figure 8. COD abatement of plasma-treated Eriochrome Black T solution.

Table 3. Stoichiometric Equation of the Dye Total Oxidation

dye	equation
Orange I	$C_{16}H_{11}N_2O_4S^- + 21O_2 \rightarrow 16CO_2 + 2NO_3^- + SO_4^{2-} + 3H^+ + 4H_2O$
Crystal Violet	$C_{25}H_{30}N_3 + 36O_2 \rightarrow 25CO_2 + 3NO_3^- + 4H^+ + 13H_2O$
Eriochrome Black T	$C_{20}H_{12}N_3O_7S^- + 25O_2 \rightarrow 20CO_2 + 3NO_3^- + SO_4^{2-} + 4H^+ + 4H_2O$

The kinetic law observed for all of the considered solutions accounts for an overall first-order process, because the plots of $\ln(COD - COD_{inf})$ vs t are linear. The plasma treatment leads to the degradation and/or mineralization of the three dyes according to the stoichiometry of the overall oxidation reactions listed in Table 3. The relevant kinetic rates are much smaller than the corresponding bleaching rates, which confirms the accepted idea[40] that bleaching is much easier than removal for the dye molecules.

Model. At the end of the bleaching period, the aromatic compounds are converted into aliphatic derivatives according to Oturan's suggestions.[41]

Guivarch et al.[40] proposed a general reaction mechanism for mineralizing azo dye molecules by oxidative action of hydroxyl radicals in the electron-Fenton process (Figure 9). The relevant mechanism involves two steps: In the first one, molecules with aromatic rings and molecular weights lower than that of the parent species are detected (e.g., hydroquinone). Additionally, the matching bleaching at the beginning of the treatment indicates that cleavage of the azo bond also occurs. In the second step, hydroxylated products such as 4-nitrocatechol, *p*-nitrophenol, pyrocatechol, and 1,4-benzoquinone were identified by several authors.[30,42] The infrared (IR) spectra indicate that the carboxylic intermediates result from the reaction between hydoxyl radicals (OH•) and aromatic rings.[43] Formic and acetic acid are known to be organic byproducts of aromatic ring-opening reactions.[44−46]

The observed decrease in the COD accounts for the mineralization process and means that the starting molecule is oxidized
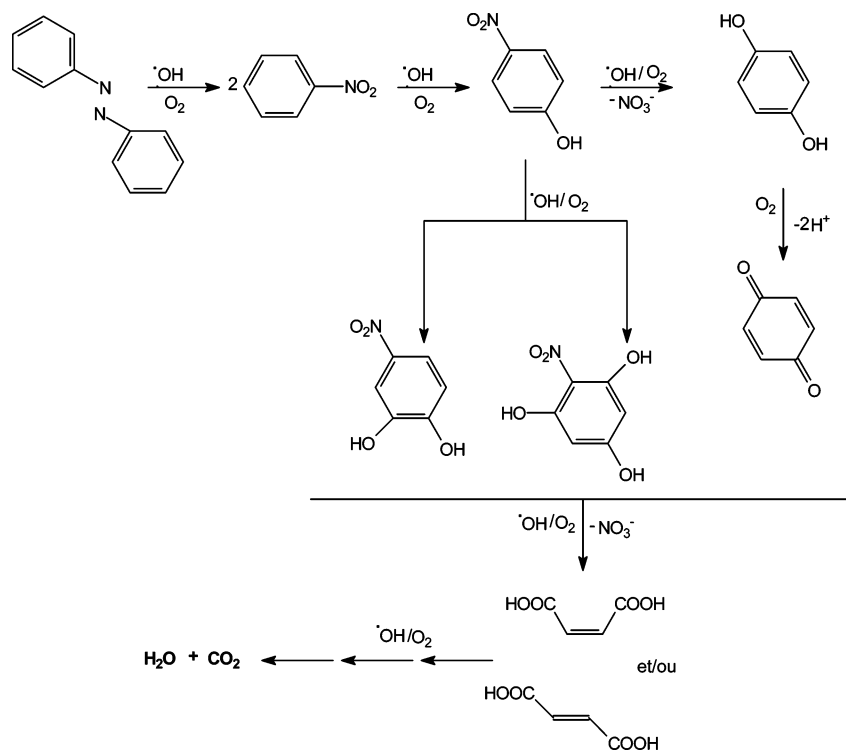
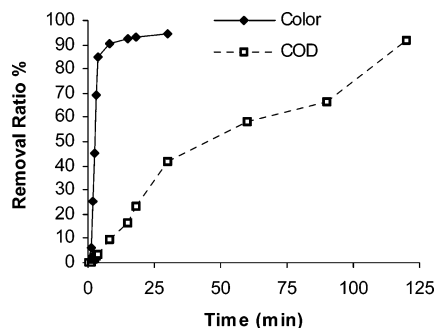**Figure 9.** Proposed reaction pathway for the mineralization of azobenzene by electron-Fenton process.

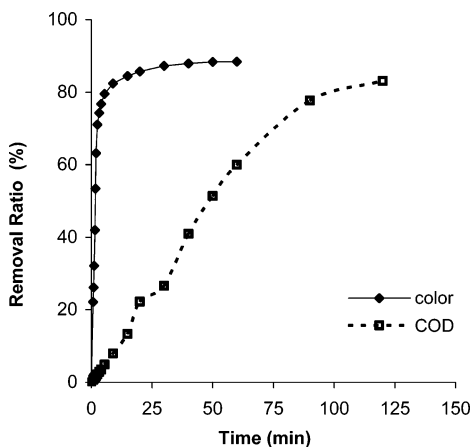**Figure 10.** Bleaching and COD removal of Orange I by the gliding arc treatment.

Figure 11. Bleaching and COD removal of plasma-treated Eriochrome black T solution.

Figure 12. Bleaching and COD removal of Crystal Violet solution by the gliding arc treatment.

to mineral ions such as NH_4^+, NO_3^-, SO_4^{2-}, CO_2, and H_2O.[47,48] Qualitative analysis of Orange I and EBT plasma-treated solutions confirmed the presence of nitrate and sulfate ions.

The occurrence of new peaks in spectral range 260−300 nm indicates the formation of new structures attributed to multi-subs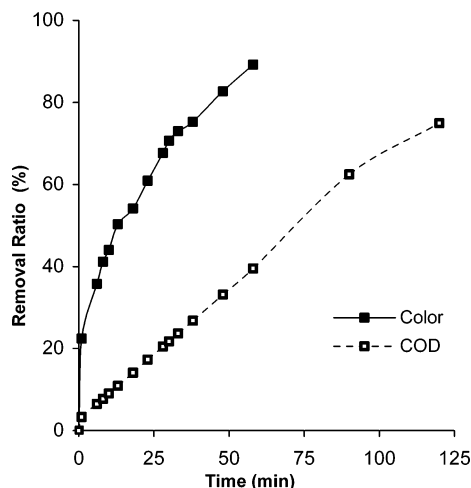tituted benzene. The presence of oxidation products such as phenol, quinone, catechol, formic acid, and acetic acid has been reported by many authors.[30,41,44]

The decrease in the chemical oxygen demand indicates the progress of mineralization; it can be explained by the conversion of the aromatic compounds into aliphatic compounds by ring-opening reactions, as already reported by different authors.[39,41,45,46] The data provided by our spectrometry and COD measurements agree satisfactorily, and they also fit well with the literature data. This leads us to accept the model proposed by Guivarch on the basis of numerous reported data.

3.3. Relationship between Bleaching and Degradation. The bleaching of the treated dye solutions matches a decrease in the COD as illustrated by Figures 10−12. The removal of the color and the COD abatement are 95% and 42%, respectively, for the Orange I solution treated for 30 min (92% for 120 min), markedly higher than for Violet Crystal solution, for which 89% and 45% (75% for 120 min) respective abatements require a 60-min plasma treatment.

The plasma-chemical treatment of Eriochrome Black T solutions causes similar effects. The bleaching and COD abatement resulting from a 60-min exposure are only 88.4% and 60%, respectively. The plasma-induced reactions are clearly much slower than for the other considered dyes. This can be related to the difference in the stability of the naphthalene and benzene structures, which is inversely related to the ease of their decomposition.

4. Conclusion

The gliding arc discharge yields a nonthermal quenched plasma at atmospheric pressure. The plasma-chemical effects of a gliding arc plasma in humid air (e.g., the oxidizing power) identified on aqueous solutions were tested on organic solutes such as aqueous solutions of various textile dyes. The reported results show that the plasma treatment is efficient and induces first the bleaching of the target solutions and then the degradation of the organic solute. Application of the gliding arc treatments to industrial wastewaters can be considered as a versatile method for the elimination of toxic chemicals and for the cleaning of industrial effluents.

Acknowledgment

Literature Cited

(1) Shen, Z.; Wang, W.; Jia, J.; Ye, J.; Feng, X.; Peng, A. Degradation of dye solution by an activated carbon fiber electrode electrolysis system. *J. Hazard. Mater.* **2001**, *B84*, 107.

(2) Cisneros, R. L.; Espinoza, A. G.; Litter, M. I. Photodegradation of an azo dye of the textile industry. *Chemosphere* **2002**, *48*, 393.

(3) Karkmaz, M.; Puzenat, E.; Guillard, C.; Herrmann, J. M. Photocatalytic degradation of the alimentary azo dye amaranth: Mineralization of the azo group to nitrogen. *Appl. Catal.* **2004**, *51*, 183.

(4) Ramakrishna, K. R.; Viraraghavan, T. Dye removal using low cost adsorbents. *Water Sci. Technol.* **1997**, *36*, 189.

(5) Nigam, P.; Armour, G.; Banat, I. M.; Singh, D.; Marchant, R. Physical removal of textile dye and solid-state fermentation of dye-adsorbed agricultural residues. *Bioresour. Technol.* **2000**, *72*, 219.

(6) O'Neill, C.; Hawkes, F. R.; Lourencou, N. D.; Pinheiro, H. M.; Delee, W. Colour in textile effluent sources. Measurement, discharge consents and simulation: A review. *J. Chem. Technol. Biotechnol.* **1999**, *74*, 1009.

(7) Arslan, I.; Balciogul, I. A.; Bahnemann, D. W. Advanced chemical oxidation of reactive dyes in simulated dyehouse effluent by ferrioxalate-Fenton/UV-A and TiO₂/UV-A processes. *Dyes Pigments* **2000**, *47*, 207.

(8) Nam, S.; Renganathan, V.; Tratnyek, P. G. Substituant effects on azo dye oxidation by the Fe^{III}−EDTA−H₂O₂ system. *Chemosphere* **2001**, *45*, 59.

(9) An, T. C.; Zhu, X. H.; Xiong, Y. Feasibility study of photoelectrochemical degradation of methylene blue with three-dimensional electrode−photocatalytic reactor. *Chemosphere* **2002**, *46*, 897.

(10) Comparelli, R.; Fanizzia, E.; Cozzoli, P. D.; Mascolo, G. Photocatalyc degradation of azo dyes by organic-capped anatase TiO₂ nanocrystals immobilized onto substates. *Appl. Catal. B: Environ.* **2005**, *55*, 81.

(11) Hasnat, M. A.; Siddiquey, I. A.; Nuruddin, A. Comparative photocatalytic studies of degradation of a cationic and anionic dye. *Dyes Pigments* **2005**, *66*, 185.

(12) Ashraf, S.; Rauf, A.; Alhadrami, S. Degradation of Methyl Red Fenton's reagent and the effect of various salts. *Dyes Pigments* **2006**, *69*, 80.

(13) Ince, N. H.; Stefan, M. I.; Bolton, J. R. UV/H₂O₂ degradation and toxicity reduction of textile azo dye: Remazol Black-B, a case study. *J. Adv. Oxid. Technol.* **1997**, *2*(3), 442.

(14) Fung, P. C.; Huang, Q.; Tsui, S. M.; Poon, C. S. Treatability study of organic and colour removal in desizing/dyeing wastewater by UV/vis system combined with hydrogen peroxide. *Water Sci. Technol.* **1999**, *40*, 153.

(15) Rott, U.; Minke, R. Overview of wastewater treatment and recycling in the textile processing industry. *Water Sci. Technol.* **1999**, *40*, 137.

(16) Stock, N. L.; Peller, J.; Vinadgopal, K.; Kamat, P. V. Combinative sonolysis and photocatalysis for textile dye degradation. *Environ. Sci. Technol.* **2000**, *34*, 1747.

(17) Benstaali, B.; Boubert, P.; Cheron, B. G.; Addou, A.; Brisset, J. L. Density and rotational temperatures measurements of the NO and OH radicals produced by a gliding arc discharge in humid air and their interaction with aqueous solutions. *Plasma Chem. Plasma Process.* **2002**, *22*, 553.

(18) Benstaali, B.; Moussa, D.; Addou, A.; Brisset, J. L. Plasma treatment of aqueous solutes: some chemical properties of a gliding arc in humid air. *Europ. Phys. J.-AP* **1998**, *4*, 171.

(19) Doubla, A.; Abdelmalek, F.; Khalifa, K.; Addou, A.; Brisset, J. L. Post-discharge plasmachemical oxidation of iron(II) complexes. *J. Appl. Electrochem.* **2003**, *33*, 73.

(20) Abdelmalek, F.; Gharbi, S.; Benstaali, B.; Addou, A.; Brisset, J.-L. Plasmachemical degradation of azo dyes by humid air plasma: yellow Supranol 4 GL, Scarlet Red Nylosan F3 GL and industrial waste. *Water Res.* **2004**, *38*, 2338.

(21) Safarik, I.; Safarikova, M. Detection of low concentration of malachite green and crystal violet in water. *Water Res.* **2002**, *36*, 196−200.

(22) Sahoo, C.; Gupta, A. K.; Anjali Pal. Photocatalytic degradation of Crystal Violet (C.I. Basic Violet 3) on silver ion doped TiO₂. *Dyes Pigments* **2005**, *66*, 189.

(23) Lesieur, H.; Czernichowski, A.; Chapelle, J. Dispositif de génération de plasmas basse température par formation de décharges électriques glissantes (Device for the formation of Low Temperature Plasmas by means of Gliding Electric Discharges). French Patent 2639172.C.A.F, 1988.

(24) Moussa, D.; Brisset, J. L.; Bargues, S. Procédé et dispositif de destruction de produits liquides par plasma froid (Process and device for the Destruction of Organic Compounds by Cold Plasma). French Patent 98-13439, 1998.

(25) Moussa, D.; Brisset, J. L. Disposal of spent tributyl phosphate by gliding arc discharge. *J. Hazard. Mater.* **2003**, *B102*, 189.

(26) Hnatiuc, E., Ed. *Procédés électriques de mesure et de traitement des polluants*; Tec & Doc Ed.: Paris, 2002.

(27) Burlica, R.; Kirkpatrick, M. J.; Finney W. C; Clark R. J.; Locke, B. R. *J. Electrostatics* **2004**, *62*, 309.

(28) Strickland, A. F.; Perkins, W. S. Decoloration of continuous dyeing wastewater by ozonation. *Textile Chem. Colorist* **1995**, *27*, 511.

(29) Bandara, J.; Morrison, C.; Kiwi, J. Degradation/decoloration of concentrated solutions of Orange II. Kinetics and quantum yield for sunlight induced reactions via Fenton type reagents. *J. Photochem. Photobio. A: Chem.* **1999**, *99*, 57.

(30) Zolinger, H. *Color Chemistry, Synthesis, Properties and Applications of Organic Dyes and Pigments*; VCH: Amsterdam, 1987.

(31) Feng, W. D.; Nansheng, H.; Helin, H. Degradation mechanism of azo dye C.I reactive red 2 by iron powder reduction and photooxidation in aqueous solution. *Chemosphere* **2000**, *41*, 1233.

(32) Vinadgopal, K.; Wynkop, D. E. Environmental photochemistry on semiconductor surfaces: photosensitized degradation of a textile azo dye, acid orange 7, on TiO₂ particles using visible light. *Environ. Sci. Technol.* **1996**, *30*, 1660.

(33) Donalgic, J.; Levec, J. Comparaison of catalyzed and non catalyzed oxidation of azo dye and effect on biodegradability. *Environ. Sci. Technol.* **1998**, *32*, 1294.

(34) Lachheb, H.; Puzenat, E.; Houas, A. Photocatalytic degradation of various types of dyes (Alizarin S, Crocein Orange G, Merthyl Red, Congo Red, Methylene Blue) in water by UV-irradiated titania. *Appl. Catal. B: Environ.* **2002**, *1025*, 1.

(35) Sahoo, C.; Gupta, A. K.; Anjali Pal. Photocatalytic degradation of Crystal Violet (C. I. Basic Violet 3) on silver ion doped TiO₂. *Dyes Pigments* **2005**, *66*, 189.

(36) Habibi, M. H.; Hassanzadeh, A.; Mahdavi, S. The effect of operational parameters on the photocatalytic degradation of three azo dyes in aqueous TiO₂ suspension. *J. Photochem.* **2005**, *172*, 89.

(37) Gupta, A. K.; Pal, A.; Sahoo, C. Photocatalytic degradation of mixture of Crystal Violet (Basic Violet 3) and Methyl Red dye in aqueous suspension using Ag⁺ doped TiO₂. *Dyes Pigments* **2006**, *69*, 224.

(38) Toor, A. P.; Verma, A.; Jotshi, C. K.; Bajpai, P. K.; Singh, V. Photocatalytic degradation of direct Yellow 12 dye using UV/TiO₂ in a Shallow pond Slurry reactor. *Dyes Pigments* **2006**, *68*, 53.

(39) Guivarch, E.; Trevin, S.; Lahitte, C..Degradation of azo dyes in water by Electro-Fenton process. *Environ. Chem. Lett.* **2003**, *1*, 38.

(40) Chun, H.; Yizhong, W. Decolourization and biodegradability of photocatalytic treated azo dyes and wool textile wastewater. *Chemosphere* **1999**, *39*, 2107.

(41) Oturan, M. A.; Oturan, N.; Lahitte, C.; Trevin, S. Production of hydroxyl radicals by electrochemically assisted Fenton's reagent. Application

to the mineralization of an organic micropollutant, pentachlorophenol. *J. Electroanal. Chem.* **2001**, *507*, 96.

(42) Joseph, J.; Destaillats, H.; Hung, H.; Hoffman, M. The sonochemical degradation of azobenzene and related azo dyes: rates enhancements via Fenton's reactions. *J Phys. Chem. A* **2000**, *104*, 301.

(43) Chen, F.; Xie, Y.; Zhao, J. Photo-Fenton degradation of dye in methanolic solution under both UV and visible irradiation. *J. Photochem. Photobiol. A: Chem.* **2001**, *138*, 139.

(44) Brillas, E.; Mur, E.; Sauledad, R.; Sanchez, L.; Peral, J.; Domenech, X. Aniline mineralization by AOP's: anodic oxidation, photocatalysis, electro-Fenton and photo-Fenton processes. *Appl. Catal. A: Environ.* **1998**, *16*, 31.

(45) Belhadj, T.; Savall, A. Mechanistic aspects of phenol electrochemical degradation by oxidation on Ta/PbO$_2$ anode. *J. Electrochem. Soc.* **1999**, *145*, 3427.

(46) Calindo, C.; Jacques, P.; Kalt A. Photodegradation of the amino-azobenzene acid orange 52 by three advanced oxidation processes: UV/H$_2$O$_2$, UV/TiO$_2$ and VIS/TiO$_2$ comparative mechanistic and kinetic investigations. *J. Photochem. Photobiol. A: Chem.* **2000**, *130*, 35.

(47) Maletzky, P.; Bauer, R. The photo-Fenton method—Degradation of nitrogen containing organic compounds. *Chemosphere* **1998**, *37*, 899.

(48) Tanaka, K.; Padermole, K.; Hisanaga, T. Photocatalytic degradation of commercial azo dyes. *Water Res.* **2000**, *34*, 327.